

Multimodal Laparoscopic System for Biological Tissue Perfusion and Metabolism Assessment

Nadezhda Golubova
R&D Center of Biomedical Photonics
Orel State University
Orel, Russia
nadin.golubova@inbox.ru

Viktor Dremin
R&D Center of Biomedical Photonics
Orel State University
Orel, Russia
College of Engineering and Physical
Sciences
Aston University
Birmingham, UK
ORCID 0000-0001-6974-3505

Elena Potapova
R&D Center of Biomedical Photonics
Orel State University
Orel, Russia
ORCID 0000-0002-9227-6308

Valery Shupletsov
R&D Center of Biomedical Photonics
Orel State University
Orel, Russia
valery.shupletsov@bmccenter.ru

Andrey Dunaev
R&D Center of Biomedical Photonics
Orel State University
Orel, Russia
ORCID 0000-0003-4431-6288

Abstract—Due to the widespread introduction of laparoscopic studies into modern surgical practice, the task of objectifying the obtained data and expanding the opportunities for obtaining additional diagnostic information is urgent. In this work, we develop the first-of-its-kind multimodal laparoscopic system integrating hyperspectral, fluorescence, and laser speckle-contrast imaging with a commercially available 5-mm rigid laparoscope. We introduced an imaging system and conducted a feasibility study on phantoms and healthy volunteers.

Keywords—*laparoscopy, hyperspectral imaging, fluorescence imaging, laser speckle-contrast imaging*

I. INTRODUCTION

Laparoscopy has low invasiveness and significantly reduces the time of the patient's postoperative stay in the hospital, thus becoming the leading approach in modern surgical practice. However, the disadvantage of standard laparoscopy is the subjectivity of intraoperative assessment of the functional state and viability of biological tissues. The expansion of the possibilities of standard laparoscopic intervention in white light using optical technologies may allow for the assessment of the morphofunctional state, perfusion and metabolic characteristics of pathological tissues.

One of the ways to improve the quality in modern clinical practice, as well as in the practice of advanced medical and biological research is the use of photonic (light-based) technologies [1]. At present, there is a broad range of lasers employed in medicine covering the spectral range from the deep ultraviolet (UV) to the mid infrared (MIR). Most medical lasers are designed to deliver a fixed amount of energy at a specific wavelength to biological tissues, causing the tissue photodynamic response. At low energies and exposure times, lasers and other types of sources become powerful diagnostic probes giving information about tissue morphology (optical coherence and optoacoustic tomography, etc.), metabolic activity (fluorescence and hyperspectral imaging), blood flow (dynamic light scattering techniques), etc. The advantages of such methods are associated with their non-invasiveness, good

resolving power, low cost and high speed and productivity. The analysis of the results of several methods of optical diagnostics can provide a huge amount of potentially useful information during minimally invasive interventions [2-5].

In this study, we demonstrate the proof-of-concept of a prototype of a multimodal laparoscope for hyperspectral [6], fluorescence [7], and laser speckle-contrast imaging [8].

II. PROTOTYPE OF MULTIMODAL LAPAROSCOPE

A 5-mm laparoscope (Richard Wolf GA-S001, Germany) is coupled to three imaging channels: hyperspectral, fluorescence, and laser speckle-contrast. Hyperspectral and fluorescence imaging modalities were constructed on the basis of the hyperspectral camera Specim IQ (Spectral Imaging Ltd., Finland), providing a spectral resolution of 7 nm within the total range of 400-1000 nm. For hyperspectral diffuse reflectance measurements, we used a homemade broadband illumination unit with a 70W halogen lamp. The fluorescence imaging channel included a blue LED source (M450LP1, Thorlabs, USA). An excitation filter is also installed in front of the source (MF445-45, Thorlabs, USA). A 500 nm long-pass filter (FELH0500, Thorlabs, USA) was placed in front of the camera to cut off the signal from the LED. Laser speckle-contrast imaging included a 785 nm laser source (LASER-785-LAB-ADJ, Ocean Insight, USA) and a CMOS monochrome camera (UI-3360CP-NIR-GL Rev 2, IDS GmbH, Germany). The 50-mm achromatic lens (AC254-050-B-ML, Thorlabs, USA) was placed in front of the camera. Preliminary studies have demonstrated that a standard laparoscope light guide is perfectly suitable for transmitting radiation of various wavelengths into the lighting channel, while maintaining not only the necessary power but also the properties of coherent radiation for the formation of a speckle pattern in the field of study.

The next section demonstrates the capabilities of the system in experiments with the developed phantoms and *in vivo* measurements on the skin of the fingers.

III. MULTIMODAL LAPAROSCOPE TESTING

A. Hyperspectral Diffuse Reflectance Imaging

We have developed elastic tissue-mimicking phantoms, using a previously developed technique [9]. In short, the

This study was supported by the Russian Science Foundation under project No. 21-15-00325.

preparation of an elastic matrix base was carried out by mixing and homogenising powdered gelatin with distilled water until a homogeneous structure is obtained. Subsequent homogenisation of the obtained solution was carried out by mixing acrylamide and bisacrylamide at room temperature. To reproduce the scattering properties, zinc oxide (ZnO) was added to the manufactured polymer structure. Subsequent polymerisation until elastic light-scattering structure was performed by adding ammonium persulfate and tetramethylethylenediamine (TEMED). A capillary with three solutions of fuchsin pigment with 20% intralipid (20, 25 and 30 μl of fuchsin per 25 ml of intralipid) was used to simulate the absorbing properties of blood.

Fig. 1a shows the registered images of a composite phantom (elastic phantom and capillary).

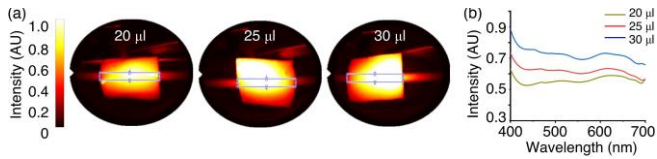


Fig. 1. Hyperspectral images of (a) phantoms and (b) diffuse reflectance spectra. ROI (blue rectangle) indicates the averaging area to obtain the spectra.

The obtained diffuse reflectance spectra from the region of interest (ROI, blue rectangle) have characteristic dips at 560 nm due to the absorption of fuchsin, and the magnitude of the dip depends on its concentration (Fig. 1b). In general, the fuchsin content increased the reflectivity of the composite phantom.

Next, the developed hyperspectral imaging channel was used to perform the finger occlusion tests in healthy volunteers. During the occlusion test, the ring finger of the right hand was occluded with a rubber band. Hyperspectral images of the intact skin during the occlusion were obtained. Finally, 2D maps of blood volume fraction, blood oxygen saturation, and indices of oxy- and deoxyhemoglobin were reconstructed using a previously developed original neural network processing [10, 11].

During the occlusion, the significant decrease in blood content was observed (Fig. 2a). Fig. 2b present the obtained maps of the blood oxygenation. The average blood oxygen level is of 80-85% for not occluded tissues. Three-minute occlusion lowers the blood oxygen content down to the level of 30-40%. Maps of the distribution of oxy- and deoxyhemoglobin indices have an inverse correlation and demonstrate a high level of deoxyhemoglobin in the occluded finger.

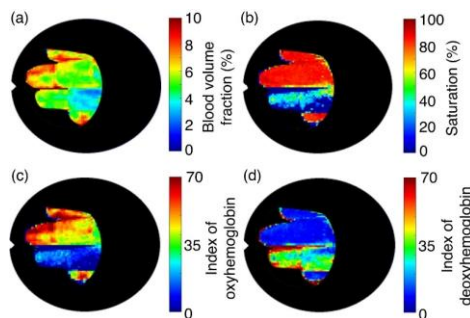


Fig. 2. Retrieved maps of (a) blood volume fraction, (b) skin blood oxygenation and indices of (c) oxy- and (d) deoxyhemoglobin during the ring finger occlusion.

B. Hyperspectral Fluorescence Imaging

To reproduce the properties of fluorescence, FAD (flavin adenine dinucleotide) was added to elastic phantoms at the manufacturing stage. Four phantoms were fabricated: without FAD and with FAD concentrations of 5, 10, 15 μmoles per 100 g of material. The acquired hyperspectral fluorescence images of four tissue-mimicking phantoms with different concentration of FAD are shown in Fig. 3a. The obtained fluorescence spectra from the ROI show the dependence of the maximum values of the fluorescence intensity on the FAD concentration in the phantom (Fig. 3b).

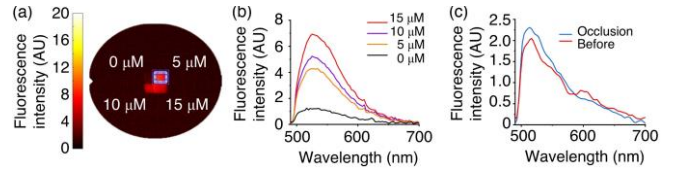


Fig. 3. Fluorescence images of (a) phantoms, obtained using a hyperspectral camera at a wavelength of 530 nm and (b) fluorescence spectra. ROI (blue rectangle) indicates the averaging area to obtain the spectra. (c) The dependence of the finger skin fluorescence spectra on the blood content.

In vivo registration of fluorescence is a non-trivial task due to the low signal level associated with its significant attenuation in the optical channel of the laparoscope. The use of the maximum exposure time of the hyperspectral camera (500 ms) and the average illumination of the finger skin surface at $0.5 \pm 0.1 \text{ mW/cm}^2$ made it possible to register hyperspectral cubes with an acceptable signal-to-noise ratio. The obtained fluorescence spectra are shown in Fig. 3c.

The blood content of tissues has a noticeable effect on the fluorescence spectra in the form of a characteristic decrease in the intensity of fluorescence at wavelengths of about 540 and 580 nm associated with the absorption of radiation by oxyhemoglobin. During the occlusion test, blood is expelled from the blood vessels, therefore, the blood filling of the tissue has less effect on the fluorescence spectrum.

C. Laser Speckle-Contrast Imaging

The test setup consists of two capillary tubes (inner diameter 1.6 mm), through which an 8% (by volume) solution of 20% intralipid was pumped using an electric pump calibrated by current/velocity. The selected 8% concentration of intralipid approximately corresponds to the optical scattering properties of blood.

To test the laser speckle-contrast system, the intralipid solution was passed through one capillary tube with linear velocities of 0.5, 1, 1.5, and 2 mm/s, which covers the *in vivo* range of blood velocities in capillaries and arterioles. The second capillary was filled with the same intralipid solution without fluid movement. The CMOS camera recorded changes in the velocity of scattering particle motion in the capillary tubes. The speckle-contrast value for each image was calculated using the standard algorithm [12, 13]. A spatial-temporal processing algorithm was used to analyze the data.

Fig. 4a shows two capillaries with an intralipid flow rate of 0 and 0.5 mm/s. The average value of the speckle-contrast was calculated in the area of 40×40 pixels in the central part of each of the capillaries (white rectangle). Statistically significant differences (Mann-Whitney *U*-test, $p < 0.05$) confirm the sensitivity of the developed channel to the motion of scattering particles (Fig. 4b).

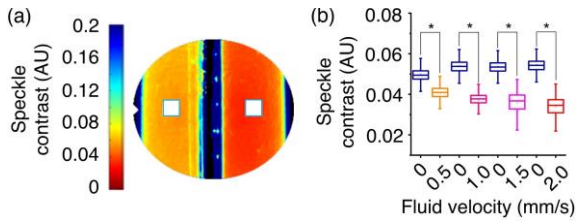


Fig. 4. (a) Speckle-contrast images of fluid motion in a capillary at 0 and 0.5 mm/s flow velocities and (b) comparison of speckle-contrast parameter between different velocities of scattering particle in the capillary tubes.

In vivo study consisted of recording speckle-contrast images before, during occlusion, and in reperfusion stage (Fig. 5). The occluded and non-occluded fingers were simultaneously placed in the field of view of the laparoscope.

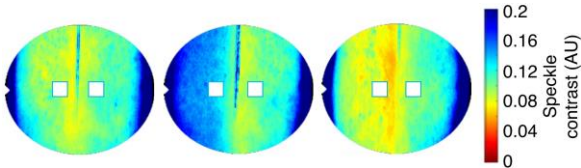


Fig. 5. Speckle-contrast images obtained before, during, and after the ring finger occlusion.

The resulting images show the response of the capillary blood flow to the occlusion and the occurrence of hyperemia after its removal, while the image corresponding to the period before the occlusion does not show a visual difference between the two fingers.

IV. CONCLUSION

We introduced an imaging system and conducted a feasibility study on phantoms and healthy volunteers. The developed system is sensitive to changes in perfusion and metabolic processes in biological tissues. Multimodal laparoscopy has a strong potential for clinical application in minimally invasive surgery. In the future, this technology could be a powerful tool for intraoperative assessment of tissue perfusion and metabolism and improved surgical decision making. Further reduction in the dimensions of hyperspectral sensors, as well as the development of image transmission technologies using fibers, can revolutionize standard laparoscopy [14, 15].

REFERENCES

[1] S. Yun and S. Kwok, "Light in diagnosis, therapy and surgery," *Nat. Biomed. Eng.*, vol. 1, p. 0008, 2017.

[2] H. Kang, S. Song, Y. Han, H.-Y. Lee, K. Kim, and S. Hong, "Proof-of-concept of a multimodal laparoscope for simultaneous NIR/gamma/visible imaging using wavelength division multiplexing," *Opt. Express*, vol. 26, no. 7, pp. 8325-8339, 2018.

[3] C. Zheng, L. Lau, and J. Cha, "Dual-display laparoscopic laser speckle contrast imaging for real-time surgical assistance," *Biomed. Opt. Express*, vol. 9, no. 12, pp. 5962-5981, 2018.

[4] E. Potapova, V. Dremin, E. Zherebtsov, A. Mamoshin, and A. Dunaev, *Multimodal Optical Diagnostic in Minimally Invasive Surgery*. Cham: Springer International Publishing, 2020, pp. 397-424.

[5] K. Kandurova, V. Dremin, E. Zherebtsov, E. Potapova, A. Alyanov, A. Mamoshin, Y. Ivanov, A. Borsukov, and A. Dunaev, "Fiber-optic system for intraoperative study of abdominal organs during minimally invasive surgical interventions," *Appl. Sci.*, vol. 9, no. 2, p. 217, 2019.

[6] G. Lu and B. Fei, "Medical hyperspectral imaging: a review," *J. Biomed. Opt.*, vol. 19, no. 1, p. 010901, 2014.

[7] M. Mycek and B. Pogue, *Handbook of Biomedical Fluorescence*. Taylor & Francis, 2003.

[8] P. Vaz, A. Humeau-Heurtier, E. Figueiras, C. Correia, and J. Cardoso, "Laser speckle imaging to monitor microvascular blood flow: a review," *IEEE Reviews in Biomedical Engineering*, vol. 9, pp. 106-120, 2016.

[9] V. Shupletsov, E. Zherebtsov, V. Dremin, A. Popov, A. Bykov, E. Potapova, A. Dunaev, and I. Meglinski, "Polyacrylamide-based phantoms of human skin for hyperspectral fluorescence imaging and spectroscopy," *Quantum Electron.*, vol. 51, no. 2, pp. 118-123, 2021.

[10] E. Zherebtsov, V. Dremin, A. Popov, A. Doronin, D. Kurakina, M. Kirillin, I. Meglinski, and A. Bykov, "Hyperspectral imaging of human skin aided by artificial neural networks," *Biomed. Opt. Express*, vol. 10, no. 7, pp. 3545-3559, 2019.

[11] V. Dremin, Z. Marcinkevics, E. Zherebtsov, A. Popov, A. Grabovskis, H. Kronberga, K. Geldnere, A. Doronin, I. Meglinski, and A. Bykov, "Skin complications of diabetes mellitus revealed by polarized hyperspectral imaging and machine learning," *IEEE Trans. Med. Imaging*, vol. 40, no. 4, pp. 1207-1216, 2021.

[12] A. Sdobnov, A. Bykov, G. Molodij, V. Kalchenko, T. Jarvinen, A. Popov, K. Kordas, and I. Meglinski, "Speckle dynamics under ergodicity breaking," *J. Phys. D: Appl. Phys.*, vol. 51, no. 15, p. 155401, 2018.

[13] E. Potapova, E. Seryogina, V. Dremin, D. Stavtsev, I. Kozlov, E. Zherebtsov, A. Mamoshin, Y. Ivanov, and A. Dunaev, "Laser speckle contrast imaging of blood microcirculation in pancreatic tissues during laparoscopic interventions," *Quantum Electron.*, vol. 50, no. 1, pp. 33-40, 2020.

[14] G. Keiser, F. Xiong, Y. Cui, and P. Shum, "Review of diverse optical fibers used in biomedical research and clinical practice," *J. Biomed. Opt.*, vol. 19, no. 8, p. 080902, 2014.

[15] P. Caramazza, O. Moran, R. Murray-Smith, and D. Faccio, "Transmission of natural scene images through a multimode fibre," *Nat. Commun.*, vol. 10, no. 1, p. 2029, 2019.